Joint analysis of area and thickness as a replacement for the analysis of cortical volume

Anderson M. Winkler[a,b,*], Douglas N. Greve[c], Knut J. Bjuland[d], Thomas E. Nichols[e], Mert R. Sabuncu[c,f], Asta K. Håberg[g,h], Jon Skranes[d,i], Lars M. Rimol[h]

[a] *Oxford Centre for Functional MRI of the Brain, University of Oxford, OX3 9DU, UK.*
[b] *Department of Psychiatry, Yale University School of Medicine, New Haven, CT, 06511, USA.*
[c] *Martinos Center for Biomedical Imaging, Massachusetts General Hospital/Harvard Medical School, Charlestown, MA, 02129, USA.*
[d] *Department of Laboratory Medicine, Children's and Women's Health, Norwegian University of Science and Technology, Trondheim, 7030, Norway.*
[e] *Department of Statistics & Warwick Manufacturing Group, University of Warwick, Coventry, CV4 7AL, UK.*
[f] *School of Electrical and Computer Engineering, and Meinig School of Biomedical Engineering, Cornell University, Ithaca, NY, 14853, USA.*
[g] *Department of Neuroscience, Norwegian University of Science and Technology, Trondheim, 7030, Norway.*
[h] *Department of Radiology, St. Olavs Hospital, Trondheim University Hospital, Trondheim, 7030, Norway.*
[i] *Department of Pediatrics, Sørlandet Hospital, 4838, Arendal, Norway.*

Abstract

Cortical surface area is an increasingly popular brain morphology metric that is ontogenetically and phylogenetically distinct from cortical thickness and offers a separate index of neurodevelopment and disease. However, the various existing methods for assessment of cortical surface area from magnetic resonance images have never been systematically compared. We show that the surface area method implemented in FreeSurfer corresponds closely to the exact, but computationally more demanding, mass-conservative (pycnophylactic) method, provided images are smoothed. Thus, the data produced by this method can be interpreted as estimates of cortical surface area, as opposed to areal expansion. In addition, focusing on the joint analysis of thickness and area, we compare an improved, analytic method for measuring cortical volume to a permutation based non-parametric combination (NPC) method. We analyze area, thickness and volume in young adults born preterm with very low birth weight, using both methods and

*Corresponding author.
Email address: winkler@fmrib.ox.ac.uk (Anderson M. Winkler)
URL: http://www.fmrib.ox.ac.uk (Anderson M. Winkler)

show that NPC analysis is a more sensitive option for studying joint effects on area and thickness, giving equal weight to variation in both of these two morphological features.

Keywords: non-parametric combination, brain cortical thickness, brain cortical area, brain cortical volume, areal interpolation

1. Introduction

It has been suggested that biological processes that drive horizontal (tangential) and vertical (radial) development of the cerebral cortex are separate from each other (Rakic, 1988; Geschwind and Rakic, 2013), influencing cortical area and thickness independently. These two indices of cerebral morphology are uncorrelated genetically (Panizzon et al., 2009; Winkler et al., 2010), are each influenced by regionally distinct genetic factors (Schmitt et al., 2008; Rimol et al., 2010b; Chen et al., 2012, 2015), follow different trajectories over the lifespan (O'Leary et al., 2007; Hogstrom et al., 2013; Fjell et al., 2015), and are differentially associated with cognitive abilities and disorders (Schnack et al., 2015; Noble et al., 2015; Lee et al., 2016; Vuoksimaa et al., 2016). Moreover, it is cortical area, not thickness, that differs substantially across species (Rakic, 1995). These findings give prominence to the use of surface area alongside thickness in studies of cortical morphology and its relationship to function. However, the literature contains a variety of approaches and terminologies for its assessment, and these have not been studied in detail or compared directly, making interpretation and comparison between studies challenging. Thus, the first objective of this paper is to compare the various methods for the analysis of cortical area currently in existence, in particular the interpolation between surfaces at different resolutions.

The second objective of this paper is to demonstrate that a statistical joint analysis of cortical thickness and surface area, using the recently proposed Non-Parametric Combination (NPC; Pesarin and Salmaso, 2010; Winkler et al., 2016b), provides a sensible solution to the investigation of

non-specific factors affecting cortical morphology. While analyzing cortical thickness and cortical area separately improves specificity over combined metrics such as cortical volume (Rimol et al., 2012), it may still be of interest to jointly analyze these two measurements so as to increase power to investigate disorders that affect thickness and area simultaneously. In principle, this could be accomplished through the analysis of cortical volume, which commingles thickness and area. Indeed, volume is a popular metric, thanks mainly to the wide use of voxel-based morphometry (VBM; Ashburner and Friston, 2000; Good et al., 2001; Douaud et al., 2007), even though a series of disadvantages have been documented (Davatzikos, 2004; Ashburner, 2009). In the traditional surface-based approach, cortical volume is measured as the product of cortical thickness and surface area at each location across the cortical mantle. However, we demonstrate that this multiplicative method incurs bias, the direction of which varies according to the local geometry of the cortex. Therefore, in order to conduct a fair comparison of surface-based cortical volume analysis and joint analysis with NPC, we propose an analytic solution to the measurement of cortical volume that does not suffer from this problem, and use this improved method when comparing cortical volume analysis to NPC.

1.1. Cortical surface area

Using continuous cortical maps to compare surface area across subjects offers considerable advantages over a region-of-interest (ROI) approach, since it does not require that the effects map onto a previously defined ROI scheme. Nevertheless, surface area analyses still depend on registration of the cortical surface and interpolation to a common resolution, and such resampling must preserve the amount of area at local, regional and global scales, i.e., it must be mass-conservative. This means that the choice of interpolation method is crucial, and our comparison will therefore focus on the interpolation between surfaces at different resolutions.

A well-known interpolation method is the *nearest-neighbour*, which can be enhanced by correction for stretches and shrinkages of the surface during the registration, as available in the function `mris_preproc`, part of the

Table 1: Overview of the four different methods to interpolate surface area and areal quantities. A detailed description is in the Materials and Methods section.

Method	**Description**
Nearest-neighbour	Nearest-neighbour interpolation of areal quantities on the sphere, followed by Jacobian correction.
Retessellation	Barycentric interpolation on the sphere of the native vertex coordinates.
Redistributive	Vertexwise redistribution of areal quantities based on barycentric coordinates of the source in relation to the target.
Pycnophylactic	Mass-conservative facewise interpolation method that uses the overlapping areas between faces of source and target.

FreeSurfer (FS) software package.[1] Another approach is the *retessellation* of the mesh of each subject to the geometry of a common grid, as proposed by Saad et al. (2004) as a way to produce meshes with similar geometry across subjects. Even though the method has been mostly used to compute areal expansion, it can be used for surface area itself, as well as for other areal quantities. A third approach is the use of the barycentric coordinates of each vertex with reference to the vertices of the common grid to *redistribute* the areal quantities, in an approximately mass conservative process. Lastly, a strategy for analysis of areal quantities using a *pycnophylactic* (mass-preserving) interpolation method, which addresses the above concerns, but that is computationally intensive, was presented in Winkler et al. (2012) (Table 1).

Few studies of cortical surface area have offered insight into the procedures adopted. Sometimes the methods were described in terms of areal expansion/contraction, as opposed to surface area itself. Furthermore, different definitions of areal expansion/contraction have been used, e.g., relative to the contra-lateral hemisphere (Lyttelton et al., 2009), to some earlier point in time (Hill et al., 2010), to a control group (Palaniyappan et al., 2011), or in relation to a standard brain, possibly the default brain (average or atlas) used in the respective software package (Joyner et al., 2009; Rimol

[1] Available at freesurfer.net

et al., 2010a, 2012; Chen et al., 2011, 2012; Vuoksimaa et al., 2016); other studies considered linear distances as proxies for expansion/contraction (Sun et al., 2009a,b). Some of the studies that used a default brain as reference did use nearest neighbor interpolation followed by smoothing, which, as we show below, assesses cortical area itself but described the measurements in terms of areal expansion (Joyner et al., 2009; Rimol et al., 2010a, 2012). Of course, measurements of areal expansion/contraction in relation to a given reference can be obtained once interpolation has been performed using the methods described here. It suffices to divide the area per face (or per vertex) by the area of the corresponding face (or vertex) in the reference brain.

1.2. Measuring volume and other areal quantities

The volume of cortical grey matter is also an areal quantity, which therefore requires mass-conservative interpolation methods. Volume can be estimated through the use of voxelwise partial volume effects using volume-based representations of the brain, such as in VBM, or from a surface representation, in which it can be measured as the amount of tissue present between the surface placed at the site of the pia mater, and the surface at the interface between gray and white matter. If the area of either of these surfaces is known, or if the area of a mid-surface, i.e., the surface running half-distance between pial and white surfaces (van Essen, 2005) is known, an estimate of the volume can be obtained by multiplying, at each vertex, area by thickness. This procedure, while providing a reasonable approximation that improves over voxel-based measurements, since it is less susceptible to various artefacts (for a discussion of artefacts in VBM, see Ashburner, 2009), is still problematic as it underestimates the volume of tissue that is external to the convexity of the surface, and overestimates volume that is internal to it; both cases are undesirable, and cannot be solved by merely resorting to using an intermediate surface as the mid-surface (Figure 1a). Here a different approach is proposed: each face of the white surface and its matching face in the pial surface are used to define an oblique truncated pyramid, the volume of which is computed analytically, without introducing additional error other than what is intrinsic to the placement and resolution of these surfaces (Figure 1b for a 2-D schema and Figure 2 for a similar in 3-D).

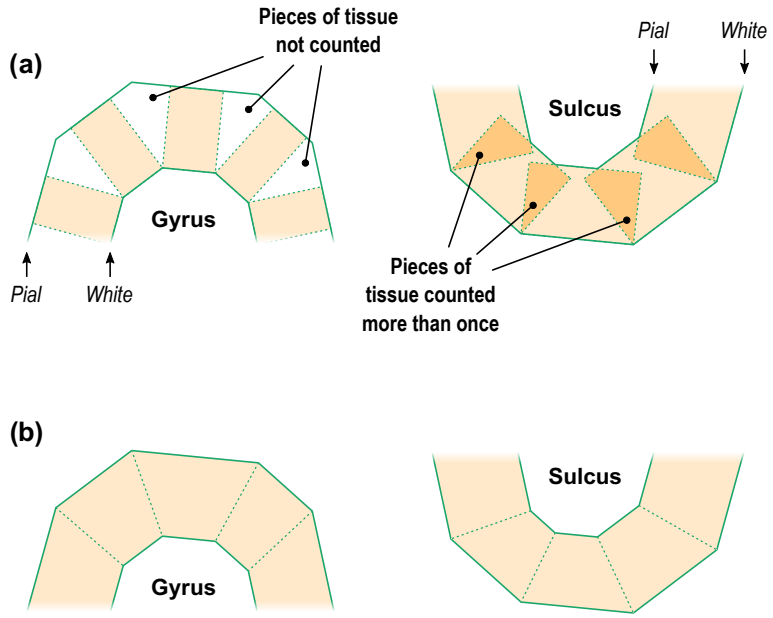

Figure 1: A diagram in two dimensions of the problem of measuring the cortical volume. (a) If volume is computed using multiplication of thickness by area, considerable amount of tissue is left unmeasured in the gyri, or measured repeatedly in sulci. The problem is minimised, but not solved, with the use of the mid-surface. (b) Instead, vertex coordinates can be used to compute analytically the volume of tissue between matching faces of white and pial surfaces, leaving no tissue under- or over-represented.

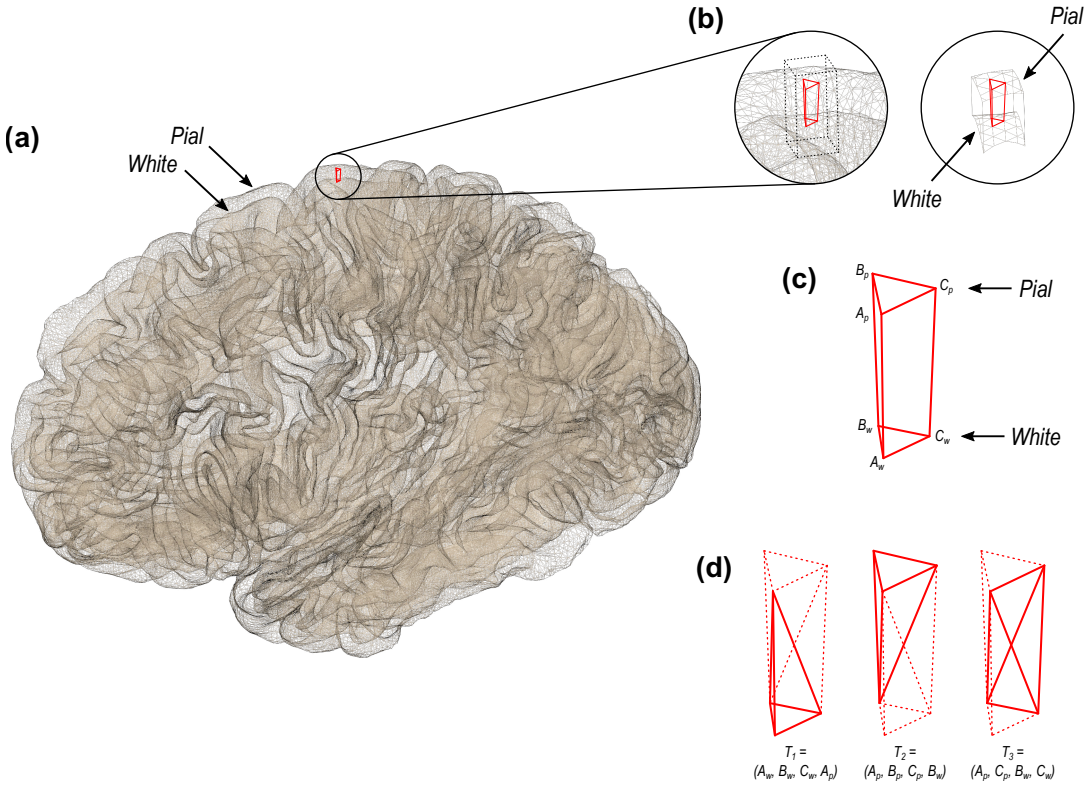

Figure 2: (*a*) In the surface representation, the cortex is limited internally by the white and externally by the pial surface. (*b*) and (*c*) These two surfaces have matching vertices that can be used to delineate an oblique truncated triangular pyramid. (*d*) The six vertices of this pyramid can be used to define three tetrahedra, the volumes of which are computed analytically.

Quantitative measurements, such as from positron emission tomography (PET), cerebral blood flow, cerebral blood volume, the mass, or number of molecules of a given compound (Leahy and Qi, 2000; van den Hoff, 2005), are all areal quantities whenever these are expressed in absolute quantities. Likewise, cerebral blood flow and volume obtained using methods based on magnetic resonance imaging (MRI), such as arterial spin labelling (ASL), as well as other forms of quantitative MRI, as those involving contrast enhancement (Parker and Padhani, 2003), quantitative magnetisation transfer (Levesque et al., 2010; Harrison et al., 2015), or quantitative assessment of myelination, are also areal quantities that require mass conservation when measured in absolute terms. The methods used for statistical analysis surface area can be applied for these areal quantities as well.

1.3. Non-parametric combination (NPC)

We argue that analysing thickness and area jointly offers important advantages over using cortical volume. Multivariate analysis of variance (MANOVA), is one such joint method, although it does not provide information about the direction of any observed effects. Rather, the permutation-based Non-Parametric Combination (NPC; Pesarin and Salmaso, 2010; Winkler et al., 2016b) supplies a test for directional as well as two-tailed hypotheses, and that is generally more powerful than MANCOVA. Moreover, it is based on minimal assumptions, mainly that of exchangeability, that is, swapping one datum for another keeps the data just as likely. The NPC consists of, in a first phase, testing separately hypotheses on each available metric using permutations that are performed in synchrony; these tests are termed *partial tests*. The resulting statistics for each and every permutation are recorded, allowing an estimate of the complete empirical cumulative distribution function (cdf) to be constructed for each one. In a second phase, the empirical p-values for each test are combined, for each permutation, into a *joint statistic*. As the joint statistic is produced from the previous permutations, all of which have been recorded, an estimate of its empirical cdf function is immediately known, and so is its corresponding p-value (Pesarin and Salmaso, 2010).

As originally proposed, and as described above, NPC is not practicable in brain imaging: since the statistics for all partial tests for all permutations need to be recorded, an enormous amount of space for data storage is necessary. However, even if storage space were not a problem, the discreteness of the p-values for the partial tests is problematic when correcting for multiple testing, because with thousands of vertices in a surface, ties occur frequently, further causing ties among the combined statistics. If too many tests across an image share the same most extreme statistic, correction for the multiplicity, while still valid, is less powerful (Westfall and Young, 1993; Pantazis et al., 2005). The most obvious workaround — run an ever larger number of permutations to break the ties — may not be possible for small sample sizes, or when possible, requires correspondingly larger data storage. The solution to this problem is loosely based on the direct combination of the test statistics, by converting the statistics of the partial tests to values

that behave as p-values using the asymptotic distribution of the statistics, and using these for the combination (Winkler et al., 2016b).

Combining functions. The null hypothesis of the NPC is that the null hypotheses for all partial tests are true, and the alternative is that any test is false, which is the same that a union-intersection test (UIT) (Roy, 1953). The rejection region depends on how the combined statistic is produced. Various combining functions can be considered, particularly those used in meta-analyses, such as Fisher's combination of p-values, i.e., $T = -2\sum_k \ln(p_k)$ (Fisher, 1932) and Stouffer's combination of z-statistics, i.e., $T = \sum_k \Phi^{-1}(1-p_k)/\sqrt{K}$ (Stouffer et al., 1949), where T is the test statistic for the joint test, p_k is the p-value of the k-th out of K partial tests, and Φ^{-1} is the probit function. These and most other combining functions, related statistics and their distributions were originally derived under the assumption of independence among the partial tests, which is not always valid, particularly under the tenable hypothesis of shared environmental effects affecting both area and thickness. Such lack of independence is not a problem for NPC: the synchronised permutations implicitly capture the dependencies among the tests that would cause a parametric combination to be invalid, even if using the same combining functions.

2. Method

The general workflow for surface-based morphometry consists of the generation of a surface-representation of the cortex and its subsequent homeomorphic transformation into a sphere. Vertices of this sphere are shifted tangentially along its surface to allow alignment matching a particular feature of interest of a reference brain (i.e., an atlas), such as sulcal depth, myelin content, or functional markers. Once registration has been done, interpolation to a common grid is performed; it is at the resolution of this grid that analyses across subjects are performed. While the order of these processing stages remains generally fixed, the stage in which areal quantities are calculated or obtained varies according to the method: for the nearest neighbour, redistributive, and pycnophylactic methods, these are computed in the native space, using native geometry. With the retessellation method,

area is computed in native space, with a new geometry produced after interpolation of the surface coordinates to the common grid. An overview of the whole process is in Figure 3; see also Supplementary Material §1. Even though here we use the FreeSurfer software package for the generation of the cortical surface and most of the preprocessing (version 5.3.0; Dale et al., 1999; Fischl et al., 1999a), broadly similar workflow and methods exist in other packages (Mangin et al., 1995; van Essen et al., 2001; Kim et al., 2005); the comparison of interpolation methods, assessment of volume, as well as NPC, are not specific to FreeSurfer.

We apply the methods to a cohort of adults born preterm with very low birth weight (VLBW) and a set of coetaneous controls. This is a particularly suitable sample for our purposes, because the neurodevelopmental brain disorders associated with preterm birth are known to have a divergent effect on cortical area and cortical thickness, including both cortical thinning and thickening (Rimol et al., 2016). Thus, a joint analysis has potential to be more informative in lieu of simple cortical volume. Using this data, we evaluate (I) whether the four different interpolation methods (nearest neighbour, retessellation, redistributive and pycnophylactic) differ; (II) whether these methods vary according to the resolution of the common grid used as target; (III) whether the two ways of measuring volume (the product method and the analytic method) differ from each other; (IV) and finally, we demonstrate some of the benefits of NPC over cortical volume when investigating group differences between VLBW and controls. We note that items (I)–(III) depend only on algorithmic and geometric differences between the methods, not interacting with particular features of this sample, such that the results of these items are generalisable.

2.1. Subjects

In the period 1986–88, 121 VLBW preterm newborns with very low birth weight; $\leqslant$ 1500g) were admitted to the Neonatal Intensive Care Unit at the St. Olav University Hospital in Trondheim, Norway. At age 20, a total of 41 VLBW subjects consented to participate and had usable MRI data. The term-born controls were born at the same hospital in the same period. A random sample of women with parities 1 or 2 was selected for follow-up

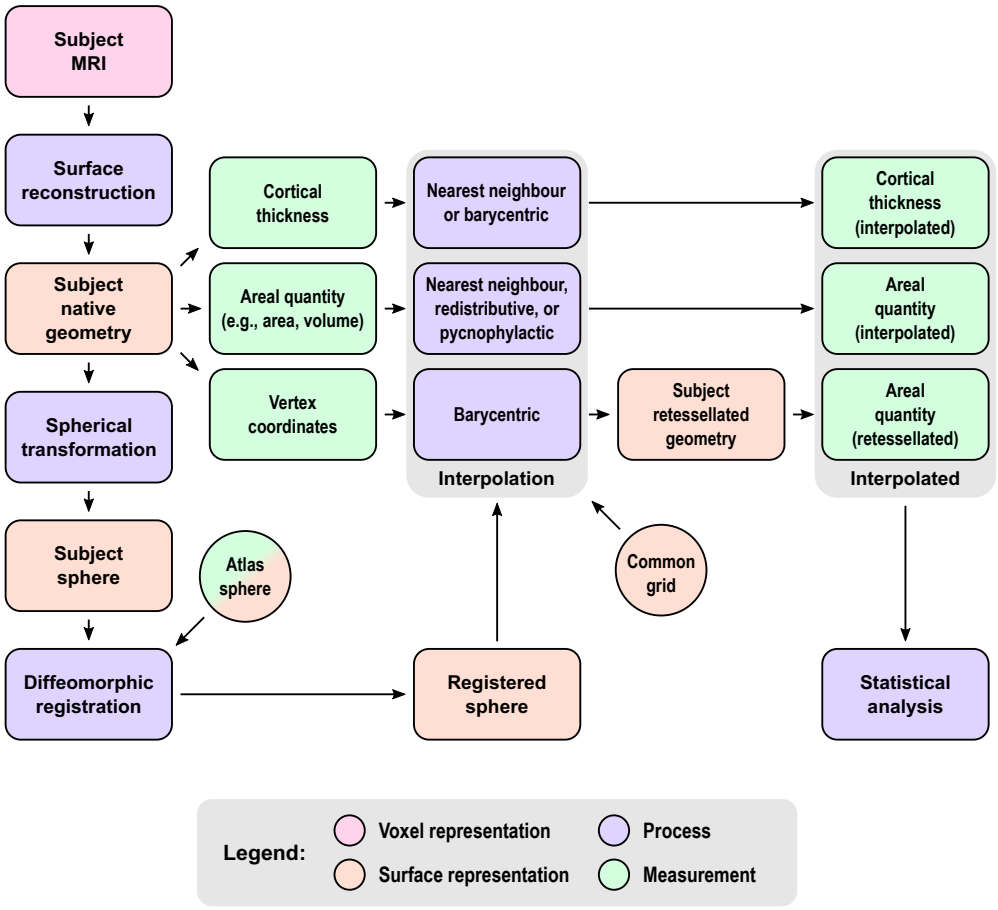

Figure 3: An overview of the steps for the analysis of surface area using different methods. The subject magnetic resonance images are used to reconstruct a pair of surfaces (pial and white) representing the cortex, which initially are in the subject space and individual geometry. From this pair of surfaces, cortical thickness can be measured. From the same surfaces, area and volume can be measured. Finally, the coordinates of the vertices can be stored for subsequent use. The subject native surfaces are homeomorphically transformed to a sphere, registered to a spherical atlas, and used for the interpolation, which for thickness can be either nearest neighbour or barycentric, for area can be nearest neighbour, redistributive or pycnophylactic, and for the vertex coordinates can be barycentric. In the latter, the interpolation of coordinates allows the construction of a new retessellated surface in subject space, from which area can alternatively be measured. The interpolated quantities are then ready to undergo statistical analyses. See references in the main text.

during pregnancy. At birth, 122 children with birth weight above the tenth percentile for gestational age from this sample were included as controls. At age 20, a total of 59 control subjects consented to participate and had usable MRI data. Further details can be found in Martinussen et al. (2005); Skranes et al. (2007). The local Regional Committee for Medical Research Ethics (Norwegian Health Region IV) approved the study protocol (REK project number: 4.2005.2605).

2.2. Data acquisition

MRI scanning was performed on a 1.5 T Siemens MAGNETOM Symphony scanner equipped with a quadrature head coil. In each scanning session, two sagittal T_1-weighted magnetization prepared rapid gradient echo (MPRAGE) scans/sequences were acquired (echo time = 3.45 ms, repetition time = 2730 ms, inversion time = 1000 ms, flip angle = 7°; field of view = 256 mm, voxel size = 1 × 1 × 1.33 mm, acquisition matrix 256 × 192 × 128).

2.3. Reconstruction of the cortical surface

T_1-weighted images are first corrected for magnetic field inhomogeneities and then skull-stripped (Ségonne et al., 2004). Voxels belonging to the white matter (WM) are identified based on their locations, on their intensities, and on the intensities of the neighbouring voxels. A mass of connected WM voxels is produced for each hemisphere, using a six-neighbours connectivity scheme, and a mesh of triangular faces is tightly built around this mass, using two triangles for each externally facing voxel side. The mesh is smoothed taking into account the local intensity in the original images (Dale and Sereno, 1993), at a subvoxel resolution. Defects are corrected (Fischl et al., 2001; Ségonne et al., 2007) to ensure that the surface has the same topological properties of a sphere. A second iteration of smoothing is applied, resulting in a realistic representation of the interface between gray and white matter (the *white surface*). The external cortical surface (the *pial surface*), which corresponds to the pia mater, is produced by nudging outwards the white surface towards a point where the tissue contrast is maximal, between gray matter and CSF, maintaining constraints on its smoothness while preventing self-intersection. Cortical thickness is measured as the distance between the matching vertices of these two surfaces (Fischl and Dale, 2000).

2.4. Measurement of areal quantities

Areal quantities are measured in native space, i.e., before spherical transformation and registration. For the retessellation method, the measurement is made in native space after the surface has been reconstructed to a particular resolution; for nearest neighbour, redistributive, and pycnophylactic, measurement uses native space, with the original, subject-specific mesh geometry.

Cortical area. For a triangular face ABC of the surface representation, with vertex coordinates $\mathbf{a} = [x_A\ y_A\ z_A]'$, $\mathbf{b} = [x_B\ y_B\ z_B]'$, and $\mathbf{c} = [x_C\ y_C\ z_C]'$, the area is $|\mathbf{u} \times \mathbf{v}|/2$, where $\mathbf{u} = \mathbf{a} - \mathbf{c}$, $\mathbf{v} = \mathbf{b} - \mathbf{c}$, $\times$ represents the cross product, and the bars $|\ |$ represent the vector norm. Although the area per face (i.e., the *facewise* area) can be used in subsequent steps, it remains the case that most software packages can only deal with values assigned to each vertex of the mesh (i.e., *vertexwise*). Conversion from facewise to vertexwise is achieved by assigning to each vertex one-third of the sum of the areas of all faces that have that vertex in common (Winkler et al., 2012).

Cortical volume. The conventional method for computing surface-based volume consists of computing the area at each vertex as above, then multiplying this value by the thickness at that vertex, in a procedure that leaves tissue under- or over-represented in gyri and sulci (Figure 1). Instead, volumes can be computed using the three vertices that define a face in the white surface and the three matching vertices in the pial surface, defining an *oblique truncated triangular pyramid*, which in turn is perfectly subdivided into three tetrahedra. The volumes of these are computed analytically, summed, and assigned to each face of the surface representation, viz.:

1. For a given face $A_wB_wC_w$ in the white surface, and its corresponding face $A_pB_pC_p$ in the pial surface, define an oblique truncated triangular pyramid.

2. Split this truncated pyramid into three tetrahedra, defined as:

$$\begin{aligned} T_1 &= (\ A_w,\ B_w,\ C_w,\ A_p\ ) \\ T_2 &= (\ A_p,\ B_p,\ C_p,\ B_w\ ) \\ T_3 &= (\ A_p,\ C_p,\ B_w,\ C_w\ ) \end{aligned}$$

   This division leaves no volume under- or over-represented.

3. For each such tetrahedra, let $\mathbf{a}$, $\mathbf{b}$, $\mathbf{c}$ and $\mathbf{d}$ represent its four vertices in terms of coordinates $[x\ y\ z]'$. Compute the volume as $|\mathbf{u} \cdot (\mathbf{v} \times \mathbf{w})|/6$, where $\mathbf{u} = \mathbf{a} - \mathbf{d}$, $\mathbf{v} = \mathbf{b} - \mathbf{d}$, $\mathbf{w} = \mathbf{c} - \mathbf{d}$, the symbol $\times$ represents the cross product, $\cdot$ represents the dot product, and the bars $|\ |$ represent the vector norm.

Computation can be accelerated by setting $\mathbf{d} = A_p$, the common vertex for the three tetrahedra, such that the vector subtractions can happen only once. Conversion from facewise volume to vertexwise is possible, and done in the same manner as for facewise area. The above method is expected to be the default in the next FreeSurfer release.

2.5. Spherical transformation

The white surface is homeomorphically transformed to a sphere (Fischl et al., 1999b), thus keeping a one-to-one mapping between faces and vertices of the native geometry (white and pial) and the sphere. All these surfaces comprise triangular faces exclusively. Measurements of interest obtained from native geometry or in native space, such as area and thickness, are stored separately and are not affected by the transformation, nor by registration (see next step; see also the diagram in Figure 3).

2.6. Registration

Various strategies are available to place all surfaces in register and allow inter-subject comparisons, including the ones used by FreeSurfer (Fischl et al., 1999b), Spherical Demons (SD) (Yeo et al., 2010), Multimodal Surface Matching (MSM) (Robinson et al., 2014), among others. Methods that are diffeomorphic (i.e., smooth and invertible) should be favoured. Methods that are not diffeomorphic by design but in practice produce invertible and

smooth warps can, in principle, be used in registration for areal analyses. In the present analyses, FreeSurfer was used; a side, complementary comparison with SD is shown in Supplementary Material §2).

2.7. Interpolation methods

Statistical comparisons require meshes with a common resolution where each point (vertex, face) represents homologous locations across individuals. One type of mesh that can act as a common grid is a geodesic sphere constructed by iterative subdivision of the faces of a regular (Platonic) icosahedron. A geodesic sphere has many advantages as the target for interpolation: ease of computation, edges of roughly similar sizes and, if the resolution is fine enough, edge lengths that are much smaller than the diameter of the sphere (Kenner, 1976). We compared four different interpolation methods each at three different mesh resolutions: IC3 (lowest resolution, with 642 vertices and 1280 faces), IC5 (intermediate resolution, with 10242 vertices and 20480 faces), and IC7 (163842 vertices and 327680 faces).

Nearest neighbour interpolation. The well known nearest neighbour interpolation does not guarantee preservation of areal quantities, although modifications can be introduced to render it approximately mass conservative: for each vertex in the target, the closest vertex is found in the source sphere, and the area from the source vertex is assigned to the target vertex; if a given source vertex maps to multiple target vertices, its area is divided between them so as to preserve the total area. If there are any source vertices that have not been represented in the target, for each one of these, the closest target vertex is located and the corresponding area from the source surface is incremented to any area already stored on it. This method ensures that total area remains unchanged after mapping onto the group surface. This process is a surface equivalent of Jacobian correction[2] used in volume-based methods in that it accounts for stretches and shrinkages while preserving

[2]Not to be confused with the computation of the Jacobian itself, that is defined, for the i-th vertex, as $J_i = \frac{A_i^S}{A_i^w} \frac{\sum_i A_i^w}{\sum_i A_i^S}$, where A_i^S is the area of the vertex in the source (registered) sphere, A_i^w is the area of the same vertex in the white surface (native space and native geometry), and the sums are over the entire surface, i.e., all vertices.

the overall amount of areal quantities. Nearest neighbour interpolation is currently the default method in FreeSurfer.

Retessellation of the native geometry. This method appeared in Saad et al. (2004). It consists of generating a new mesh by interpolating not the area assigned to vertices but the coordinates of the corresponding vertices in the native geometry. The set of three coordinates is used, together with the connectivity scheme between vertices from the common grid, to construct a new mesh that has similar overall shape as the original brain, but with the geometry of the common grid. The area for each face (or vertex) can be computed from this new mesh and used for statistical comparison across subjects. Equivalently, the coordinates of each vertex can be treated as a single vector and the barycentric interpolation can be performed in a single step, as:

$$\begin{bmatrix} x_P \\ y_P \\ z_P \end{bmatrix} = \begin{bmatrix} x_A & x_B & x_C \\ y_A & y_B & y_C \\ z_A & z_B & z_C \end{bmatrix} \begin{bmatrix} \delta_A \\ \delta_B \\ \delta_C \end{bmatrix}$$

where x, y, z represent the coordinates of the triangular face ABC and of the interpolated point P, both in native geometry, and δ are the barycentric coordinates of P with respect to the same face after the spherical transformation. From the four methods considered in this chapter, this is the only one that does not directly interpolate either area or areal quantities, but the mesh in native space.

Redistribution of areas. This method works by splitting the areal quantity present at each vertex in the source sphere using the proportion given by the barycentric coordinates of that vertex in relation to the face in the target sphere (common grid) on which it lies, redistributing these quantities to the three vertices that constitute that face in the target. If some quantity was already present in the target vertex (e.g., from other source vertices lying on the same target face), that quantity is incremented. The method is represented by:

$$Q_i^T = \sum_{f=1}^{F} \sum_{v=1}^{V_f} Q_{vf}^S \delta_{ivf}$$

where Q_{vf}^S is the areal quantity in the source vertex v, $v \in \{1, \ldots, V_f\}$ lying on the target face f, $f \in \{1, \ldots, F\}$, F being the number of faces that meet at the target vertex i, and δ_{ivf} is the barycentric coordinate of v, lying on face f, and in relation to the target vertex i. This method has similarities with the conventional barycentric interpolation (as used for the interpolation of coordinates in the retesselation method). The key difference is that in the barycentric interpolation, it is the barycentric coordinates of the target vertex in relation to their containing source face that are used to weight the quantities, in a process that therefore is not mass conservative. Here it is the barycentric coordinates of the source vertex in relation to their containing target face that are used; the quantities are split proportionately, and redistributed across target vertices.

Pycnophylactic interpolation. The ideal interpolation method should conserve the areal quantities globally, regionally and locally. In other words, the method has to be *pycnophylactic*. This is accomplished by assigning, to each face in the target sphere, the areal quantity of all overlapping faces from the source sphere, weighted by the fraction of overlap between them (Markoff and Shapiro, 1973; Winkler et al., 2012). The pycnophylactic method operates on the faces directly, not on vertices and the area (or any other areal quantity) is transferred from source to target surface via weighting by the overlapping area between any pairs of faces. The interpolated areal quantity, Q_i^T, of a face i in the target surface, that overlaps with F faces from the source surface, is given by:

$$Q_i^T = \sum_{f=1}^{F} \frac{A_f^O}{A_f^S} Q_f^S$$

where A_f^S is the area of the f-th overlapping face from the source sphere, which contains a quantity Q_f^S of some areal measurement (such as the surface area measured in the native space), and A_f^O is the overlapping area with the face i.

Correction for unequal face sizes and smoothing. Regardless of the interpolation method used, larger faces in the common grid inherit larger amounts of areal quantities. If the analysis will compare regions that are topographically distinct, or if the data are to be smoothed, a correction for different face sizes is needed (Winkler et al., 2012). For facewise data, such a correction consists of weighting the areal quantity at each face or vertex, after interpolation, by a constant that depends on the respective area in the common grid. Smoothing was considered at two levels for the comparison of areal interpolation and volume methods: no smoothing, and smoothing with a Gaussian kernel with full width at half maximum (FWHM) of 10 mm, small so as to preserve the effect of different resolutions being investigated. For the comparison between VLBW and controls, 30 mm, as in Rimol et al. (2016).

2.8. Statistical analysis

The statistical analysis was performed using PALM – Permutation Analysis of Linear Models (Winkler et al., 2014, 2016b). The number of permutations was set to 1000, followed by approximation of the tail of the distribution by a generalised Pareto distribution (GPD; Winkler et al., 2016a), and familywise error rate correction (FWER) was done considering both hemispheres and both test directions for the null hypothesis of no difference between the two groups. Analyses were performed separately for cortical thickness, area, and volume (both methods), and also using NPC for the joint analysis of thickness and area; Figure 4 shows an overview of how these are related.

3. Results

3.1. Preservation of areal quantities

All methods preserve generally well the global amount of surface area, and therefore, of other areal quantities, at the highest resolution of the common grid (IC7). At lower resolutions, massive amounts of area are lost with the retessellation method: about 40% on average for IC3 (lowest resolution, with 642 vertices and 1280 faces) and 9% for IC5 (intermediate resolution, with 10242 vertices and 20480 faces), although only 1% for IC7 (163842 vertices and 327680 faces). Areal losses, when existing, tend to be uniformly

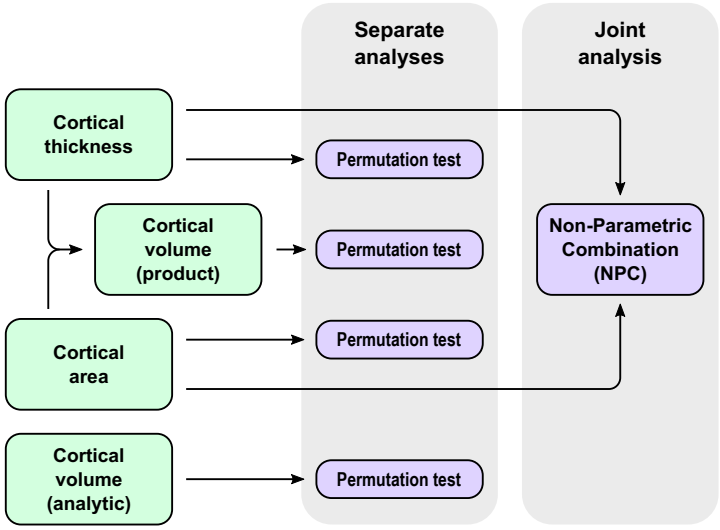

Figure 4: Overview of the separate and joint analyses of thickness, area and volume.

distributed across the cortex (Figure 5, upper panels), with no trends affecting particular regions and, except for retessellation, can be substantially alleviated by smoothing. With the latter, areal losses accumulate throughout the cortex, and the global cortical area, if computed after interpolation, becomes substantially reduced (biased downwards), even at the highest resolution of the common grid. An extended set of results that support these findings is shown in the Supplementary Material §2.

3.2. Differences between interpolation methods

While there are no spatial trends in terms of areal gains or losses, the inexactness of the non-pycnophylactic interpolation methods introduces noise that substantially reduces their correlation when assessed between subjects (Figure 5, lower panels). The only exception is between the retessellation and the pycnophylactic method, which have near perfect correlation even without any smoothing. Smoothing increases the correlation between all methods to near unity throughout the cortex (Supplementary Material §2a). At the subject level, the spatial correlation between the nearest neighbour and the pycnophylactic method is only about 0.60, although approaching unity when the subjects are averaged (Supplementary Material §2b). Smoothing leads to a dramatic improvement on agreement, causing nearest neighbour to be nearly indistinguishable from the pycnophylactic method. The redistributive method performed in a similar manner, although with a higher correlation without smoothing, i.e., about 0.75 (Supplementary Material §2b).

Figure 5: *(page 21)* Pairwise average differences (in mm^2) and correlations between the four interpolation methods, using the IC7 as target, with or without smoothing with a Gaussian kernel of FWHM = 10 mm, projected to the average white surface. Although the four methods differ, with some leading to substantial, undesirable losses and gains in surface area, and the introduction of noise manifested by lower correlations, the average variation was zero for nearest neighbour, redistributive and pycnophylactic. The retessellation method led to substantial losses of area that could not be recovered or compensated by blurring. Although this method showed excellent correlation with pycnophylactic, quantitative results after interpolation are biased downwards. For the medial views, for the right hemisphere, for IC3 and IC5, and for projections to the pial and inflated surfaces, consult the Supplemental Material.

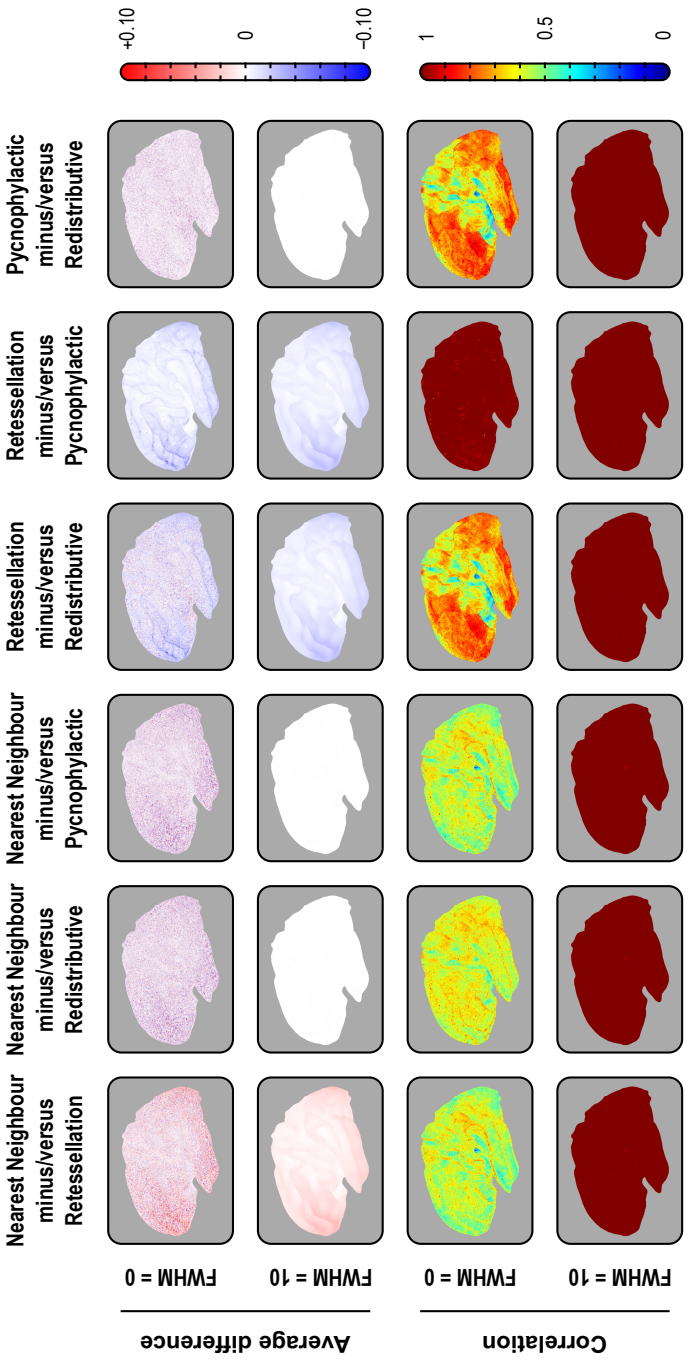

3.3. Cortical volume measurements

At the local scale, differences between the product and the analytic methods of volume estimation are as high as 20% in some regions, an amount that could not be alleviated by smoothing or by changes in resolution. As predicted by Figure 1, differences were larger in the crowns of gyri and depths of sulci, in either case with the reverse polarity (Figure 6, upper panels). The vertexwise correlation between the methods across subjects, however, was in general very high, approaching unity throughout the whole cortex, with or without smoothing, and at different resolutions. In regions of higher sulcal variability, however, the correlations were not as high, sometimes as low as 0.80, such as in the insular cortex and at the confluence of parieto-occipital and calcarine sulci, between the lingual and the isthmus of the cingulate gyrus (Figure 6, lower panels). At least in the case of the insula, this effect may be partly attributed to a misplacement of the white surface in the region lateral to the claustrum (Glasser et al., 2016). Supplementary Material §3 includes additional results that support these findings.

3.4. Global measurements and their variability

Average global cortical area, thickness, and volume (using both methods) across subjects in the sample are shown in Table 2. Cortical volumes assessed with the multiplicative method are significantly higher ($p < 0.0001$) than using the analytic method. Variability for area is higher than for thickness, and even higher for volume: the average coefficient of variation across subjects ($100 \cdot \sigma/\mu$) was, respectively, 9.9%, 3.2% and 10.5%, after adjusting for group, age, and sex, with the parietal region (bilateral) being the most variable for all measurements. The corresponding spatial maps are shown in Figure 7; for scatter and Bland–Altman plots, see Supplementary Material §4.

3.5. Differences between VLBW and controls

Analysing cortical thickness and area separately, the comparisons between the VLBW subjects and the controls suggest a distinct pattern of significant differences ($p \leqslant 0.05$, FWER-corrected). Surface area maps show

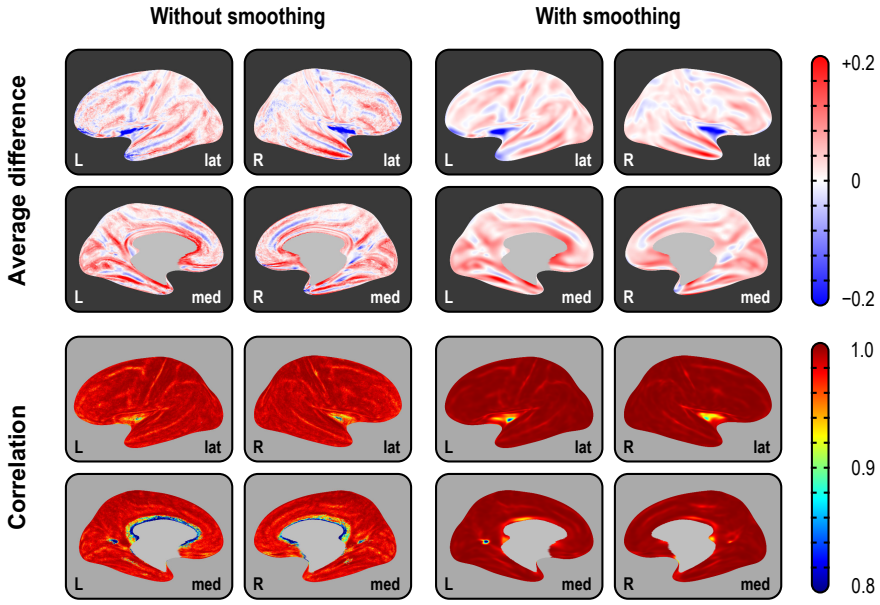

Figure 6: Average difference (in mm^3) between the two methods of assessing volume and their correlation (across subjects), using the highest resolution (IC7) as the interpolation target, projected to the average inflated surface. As predicated from Figure 1, differences are larger in the crowns of gyri and in the depths of sulci, with gains/losses in volume in these locations following opposite patterns. Although the correlations tend to be generally high, and increase with smoothing, they are lower in regions of higher inter-individual morphological variability, such as at the anterior end of the cuneus, and in the insular cortex. For IC3 and IC5, and for projections to the white and pial surfaces, consult the Supplemental Material.

Table 2: Average ± standard deviation of area (in mm^2), thickness (in mm) and volume (in mm^3) across subjects. Volumes are shown assessed using the multiplicative (m) and analytic (a) methods; their difference is also shown.

Measure	Left hemisphere	Right hemisphere	Both hemispheres
Area	97104.3 ± 9594.8	97767.7 ± 9684.4	194872.0 ± 19247.6
Thickness	2.5357 ± 0.0951	2.5273 ± 0.0914	2.5314 ± 0.0921
$\text{Volume}^{(m)}$	246268.9 ± 26416.7	247131.0 ± 26529.9	493399.9 ± 52855.7
$\text{Volume}^{(a)}$	242580.3 ± 26141.4	243688.3 ± 26214.0	486268.6 ± 52266.3
$\text{Difference}^{(m-a)}$	3688.6 ± 569.2	3442.7 ± 605.8	7131.4 ± 1087.2

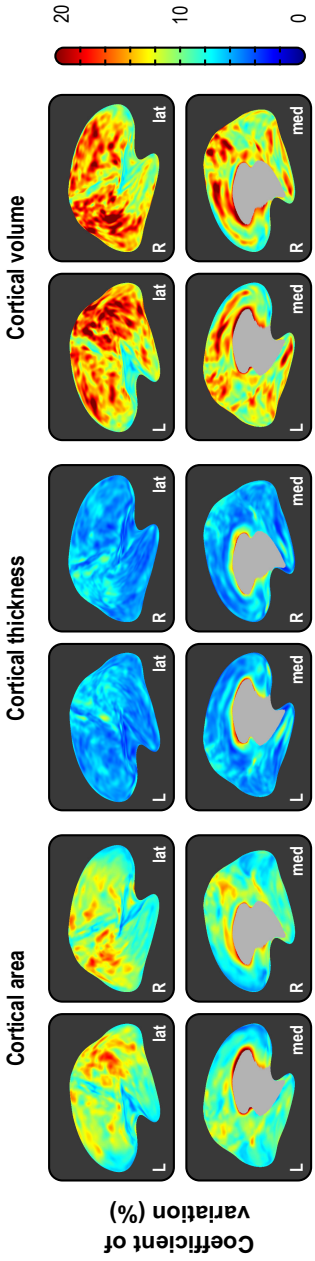

Figure 7: Coefficient of variation (σ/μ) after regressing the variability due to age, sex, and group. The variability across subjects is higher for area than for thickness, and even higher for volume. In all cases, the parietal cortex (parietal) is the region with the highest variability. For projections to the white and pial surfaces, consult the Supplemental Material.

a significant bilateral reduction in the middle temporal gyrus, the superior banks of the lateral sulcus, and the occipito-temporal lateral (fusiform) gyrus, as well as a diffuse bilateral pattern of areal losses affecting the superior frontal gyrus, posterior parietal cortex and, in the right hemisphere, the subgenual area of the cingulate cortex. Cortical thickness maps show a diffuse bilateral thinning in the parietal lobes, left middle temporal gyrus, right superior temporal sulcus, while showing bilateral thickening of the medial orbito-frontal cortex and the right medial occipital cortex of the VLBW subjects compared to controls (Figure 8, upper panels, light blue background). Maps of cortical volume differences largely mimic the surface area results, albeit with a few differences: diffuse signs of volume reduction in the parietal lobes, ascribable to cortical thinning and, contrary to the analysis of area and thickness, no effects found in the medial-orbitofrontal or in the subgenual region of the cingulate gyrus (Figure 8, middle panels, light red background).

3.6. Joint analysis via NPC

Non-parametric combination of thickness and area provides information about patterns of group differences not visible in cortical volume analyses (Figure 8, lower panels, light green background). In the present data, the

Figure 8: *(page 27)* Separate (*light blue background*) and joint (*green*) analysis of cortical area and thickness, as well as volume (*red*), using the IC7 resolution and smoothing with FWHM = 30mm. Analysis of area indicates no increases in the VLBW group anywhere in the cortex (A), and reductions in, among other regions, the subgenual region of the cingulate cortex (B). Analysis of thickness indicates that VLBW subjects have thicker cortex in the medial orbitofrontal cortex (C) and in the right medial occipital cortex, as well as diffuse bilateral thinning in parietal and middle temporal regions (D). Analysis of volume alone broadly mimics analysis of area, with no evidence of increased volume in VLBW subjects (E), although in some maps there seems to be a partial superimposition of the effects seen separately for area and thickness, with signs of bilaterally decreased volume throughout the parietal lobe (F), but contrary to the analysis of area, no signs of reduction in the subgenual cortex (G). Jointly analysing area and thickness gives equal weight to both measurements, and allows directional effects to be inferred. Contrary to the case for volume, it is possible to know that there is an increase in the amount of cortical tissue in VLBW subjects in the medial orbito-frontal cortex (H) when compared to controls, and a bilateral decrease throughout most of the parietal cortex, stronger in the middle temporal and fusiform gyri, in both hemispheres (I). Moreover, the joint analysis allows search for effects that can negate each other, such as in this case weaker effects in the parietal region (J), that partially overlap in space with those shown in (I). Finally, strong effects in the middle orbitofrontal, that were missed with simple volumes (G) become clearly visible (K).

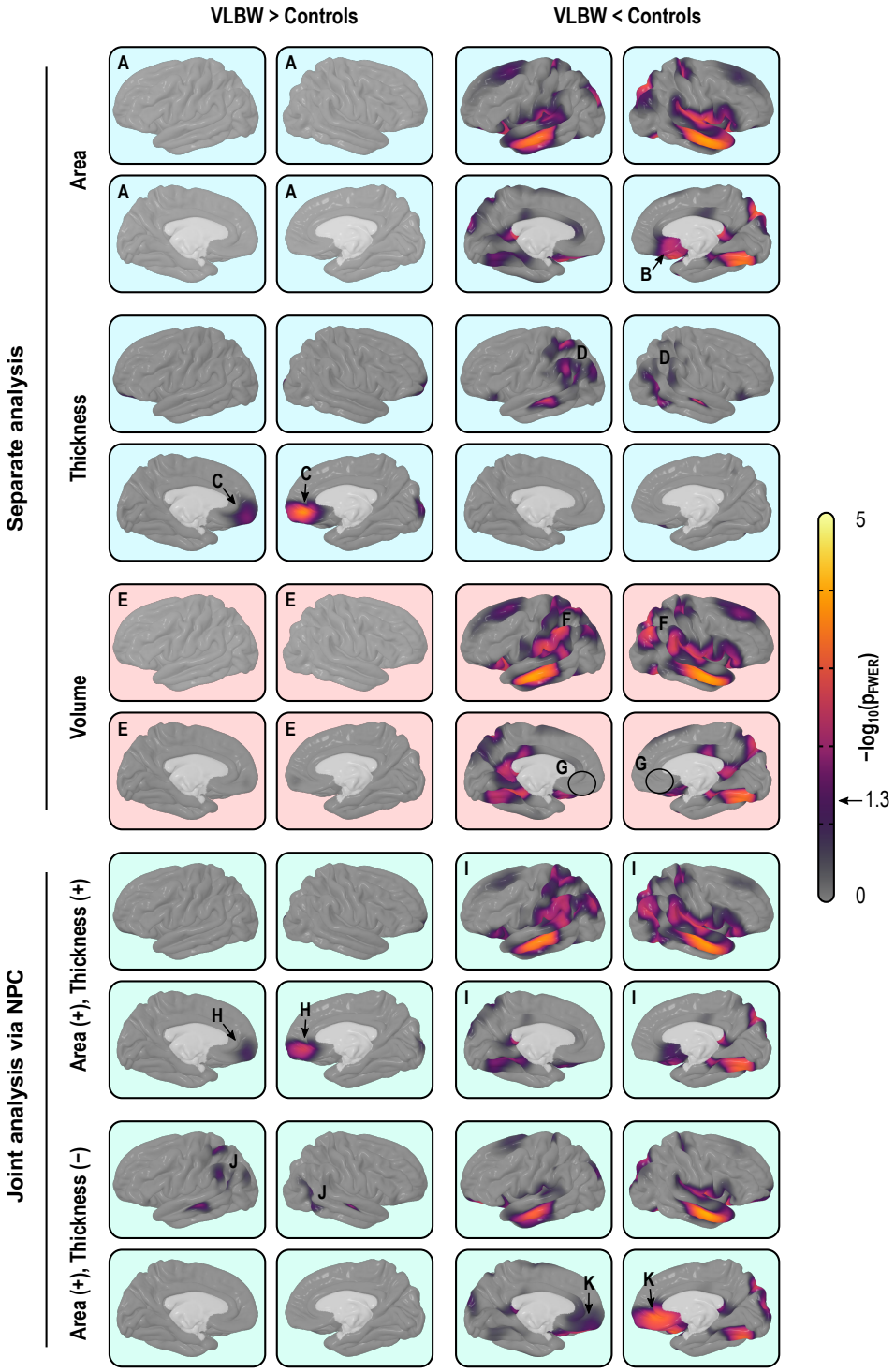

joint analysis suggests a decrease in the amount of tissue in VLBW subjects in the medial orbito-frontal cortex, which is not visible in the volume analysis, as well as a bilateral decrease throughout most of the parietal cortex, and in the middle temporal and fusiform gyri. Finally, NPC shows simultaneous bilateral decrease in surface area and increase in thickness in the medial orbito-frontal gyrus, none of which was observed using simple volume measurements. For additional maps, see Supplementary Material §5.

4. Discussion

4.1. Interpolation of areal quantities

The different resampling methods do not perform similarly in all settings. Nearest neighbour and redistributive require smoothing of at least FWHM = 10 mm as used here in order to become comparable to, and interchangeable with, the pycnophylactic method. However, since data is usually smoothed in neuroimaging studies in order to improve the matching of homologies and to improve the signal-to-noise ratio, this is not a significant limitation. Retessellation, particularly at lower resolutions, leads to substantial areal losses that cannot be recovered even with smoothing. Moreover, the vertices of the retessellated surfaces are not guaranteed to lie at the tissue boundaries they represent, introducing uncertainties to the obtained measurements. Regarding speed, although the various implementations run on linear time, $\Theta(n)$, the pycnophylactic method has to perform a larger number of computations that may not pay off when compared with nearest neighbour, provided that smoothing is used.

4.2. Volumes improved, yet problematic

The large absolute difference between the product and the analytic method for cortical volume indicates that if interest lies in the actual values (for instance, for predictive models), the analytic method is to be preferred. The high correlation across subjects, however, suggests that, for group comparisons and similar analyses, both methods generally lead to similar results, except in a few regions of higher morphological inter-individual variability. However, even in these cases, cortical volume is a poor choice of trait of

interest. Even though volume encapsulates information on both area and thickness, research has suggested that the proportion in which the variability of these two measurements coalesces varies spatially across the cortical mantle (Winkler et al., 2010; Storsve et al., 2014). Moreover, previous literature suggests that most of the between-subject variability of cortical volume, including that measured using VBM, can be explained by the variability of surface area (Voets et al., 2008; Lenroot et al., 2009; Winkler et al., 2010; Rimol et al., 2012), whereas most of the within-subject variability can be explained by variability of cortical thickness (Storsve et al., 2014), thus rendering volume a largely redundant metric. In effect, the continuous cortical maps in Figure 5, resulting from a between-subject analysis, confirm that the results for cortical volume largely mirror the results for cortical surface area.

4.3. Joint analyses via NPC

Such problems with cortical volume can be eschewed through the use of a joint statistical analysis of area and thickness. The NPC methodology gives equal (or otherwise predefined) weights for thickness and area, which therefore no longer have their variability mixed in unknown and variable proportions across the cortical mantle. Various combining functions can be considered, and the well-known Fisher method of combination of p-values (Fisher, 1932) is a simple and computationally efficient choice. By using two distinct metrics in a single test, power is increased (Fisher, 1932; Pesarin and Salmaso, 2010; Winkler et al., 2016b), allowing detection of effects that otherwise may remain unseen when analysing volume, or when thickness and area are used separately. NPC can be particularly useful for the investigation of processes affecting cortical area and thickness simultaneously, even if in opposite directions or at different rates (both phenomena that have been recently reported, e.g., Hogstrom et al., 2013; Storsve et al., 2014), and can effectively replace volume as the measurement of interest in these cases, with various benefits and essentially none of the shortcomings. It constitutes a general method that can be applied to any number of partial tests, each relating to hypotheses on data that may be of a different nature, obtained using different measurement units, and related to each other arbitrarily.

Moreover, NPC allows testing specific directional hypotheses (by reversing the signs of partial tests), hypotheses with concordant directions (taking the extremum of both after multiple testing correction), and two-tailed hypotheses (with two-tailed partial tests). Power increases consistently with the introduction of more partial tests when there is a true effect, while strictly controlling the error rate. This is in stark contrast to classical multivariate tests based on regression, such as MANOVA or MANCOVA, that do not provide information on directionality of the effects, and lose power as the number of partial tests increase past a certain optimal point.

A joint test using NPC has similarities with, yet it is distinct from, the test known as *conjunction* or *intersection-union test* (IUT) (Nichols et al., 2005). The NPC tests a joint null hypothesis that all partial tests have no effect; if the null is rejected in any partial test at a suitable level, the joint null is rejected. The conjunction tests a null hypothesis that at least one partial test has no effect; the alternative is that all partial tests have an effect. While a conjunction seeks an effect across all tests, NPC seeks an effect in any, or in an aggregate of the partial tests. Usage of NPC is not constrained to the replacement of cortical volume, and the method can be considered for analyses involving other cortical indices, including myelination (Glasser and Van Essen, 2011; Sereno et al., 2013) and folding and gyrification metrics (Mangin et al., 2004; Schaer et al., 2008; Toro et al., 2008) that can interact in distinct and complex ways (Tallinen et al., 2014, 2016), among others.

4.4. Permutation inference

Permutation tests provide exact inference based on minimal assumptions, while allowing multiple testing correction with strong control over the error rate. Even though permutation tests still have certain requirements, such that the data are exchangeable, certain types of structured dependency can be accommodated by means of restricted permutation strategies. Being based on permutations in each of the partial tests, NPC does not preclude the analysis of thickness and area (or of other partial tests) separately, and through the synchronised shuffling, correction for multiplicity of tests while taking into account their non-independence is trivial. This includes correction for multiple tests that may be used using various combinations

of positive and negative directions for the partial tests. Permutation tests do not depend on distributional assumptions, which favours the analysis of surface area, which at the local level shows positive skewness, and is better characterised as log-normal (Winkler et al., 2012).

4.5. Area and thickness of VLBW subjects

The reduced cortical surface area observed in VLBW subjects compared to controls replicates previous findings from the same cohort at 20 years of age (Skranes et al., 2013), and is consistent with findings from a younger cohort of VLBW subjects (Sølsnes et al., 2015) and teenagers born with extremely low birth weight ($\leqslant$ 1000g) (Grunewaldt et al., 2014). The combined evidence from these studies suggests that surface area reductions in the preterm brain are present from early childhood and remain reasonably constant from childhood until adulthood (Rimol et al., 2016). Proposed mechanisms for gray matter injury in preterm birth include hypoxia-ischemia and inflammation arising from intrauterine infections or from postnatal sepsis (Volpe, 2009, 2011), which may adversely affect critical phases of brain maturation before and after birth and cause diffuse white matter damage, including hypomyelination and primary or secondary gray matter dysmaturation (Hagberg et al., 2015). Cortical area reductions may not be explained by primary white matter damage alone, especially since area reductions are also observed in younger cohorts of preterms with less perinatal morbidity and less pathology in white matter microstructure, evaluated with diffusion tensor imaging (Eikenes et al., 2011; Rimol et al., 2016). Reduced neuropil is a possible explanation for cortical thinning in the lateral parietal and temporal cortex in VLBW subjects, but the thickening of the medial orbito-frontal cortex must be due to different mechanisms (Marín-Padilla, 1997; Bjuland et al., 2013; Grunewaldt et al., 2014). The combination of thickening and reduced area in medial orbito-frontal cortex has been observed in multiple cohorts and, more generally, these changes in both thickness and area could be related to prenatal factors, such as foetal growth restriction, or to postnatal exposure to extra-uterine environmental stressors (Sølsnes et al., 2015; Rimol et al., 2016). Regardless of underlying pathological aspects, the morphological indices appear to be robust markers of perinatal brain injury and

maldevelopment (Raznahan et al., 2011; Skranes et al., 2013; Rimol et al., 2016).

4.6. Limitations

Since NPC is based on permutation tests, it is a requirement that the assumption of exchangeability holds, which can be a limitation when dependencies between observations cannot be fully accounted for by the model. In addition, the method can be computationally intensive, particularly for large datasets, or datasets using high resolutions. Both problems can be solved, at least in particular cases: structured dependencies (such as when studying twins) can be accommodated using restricted permutation schemes (Winkler et al., 2015), whereas permutation tests can be accelerated using various approximate or exact methods (Winkler et al., 2016a); the latter was used in this particular analysis.

The present VLBW sample is medium-sized and it is possible that real but undetected group effects, including volume differences, would appear as significant in a larger sample. However, to the extent that cortical thickness and surface area go in opposite directions, e.g. increased thickness and reduced area in one of the groups, as observed in the medial anterior superior frontal gyrus and orbitofrontal cortex in the present sample, failure to detect group differences in cortical volume can be unrelated to statistical power issues.

5. Conclusion

We studied the four extant interpolation methods for the assessment of cortical area, and observed that the nearest neighbour interpolation, followed by a Jacobian correction and smoothing, is virtually indistinguishable from the pycnophylactic method, albeit with reduced computational costs. This leads us to recommend, for practical purposes, the nearest neighbour method, with smoothing, when investigating cortical surface area. In addition, we demonstrate that the non-parametric combination of cortical thickness and area can be more informative than a simple analysis of cortical volume, even when the latter is assessed using the improved, analytic

method that does not over or under-represent tissue according to the cortical convolutions.

Supplementary Material

The large number of scenarios evaluated, that involved two different registration and four different interpolation methods, three grid resolutions, two different smoothing levels, four different indices of cortical morphology, plus NPC, resulted in more than 16 thousand maps and Bland–Altman plots (Bland and Altman, 1986). These have been organised in a set of browsable pages that constitutes the Supplementary Material, and that can be found at **http://bit.ly/2cHJFQC**. The results above make ample reference to this material, and its inspection is encouraged. The Supplementary Material also includes high resolution and complementary views of all figures shown in the main text.

Acknowledgements

The authors thank Donald J. Hagler Jr. (University of California, San Diego, CA, USA), and David Van Essen and Matthew F. Glasser (Washington University Medical School, St. Louis, MO, USA) for the helpful discussions at different stages of this work. This research project was supported by grants from the Research Council of Norway (ES182663) and the Central Norway Regional Health Authority (46056610 and 46039500). A.M.W. is supported by the National Research Council of Brazil (CNPq; 211534/2013-7). T.E.N. is supported by the Wellcome Trust (100309/Z/12/Z). M.R.S. received funding from the NIH R21AG050122-01A1, R41AG052246-01 and 1K25EB013649-01 projects. Data processing was largely performed on the Abel Cluster, owned by the University of Oslo and the Norwegian Metacenter for High Performance Computing (NOTUR), and operated by the Department for Research Computing at USIT, University of Oslo.

References

Ashburner, J., 2009. Computational anatomy with the SPM software. Magn Reson Imaging 27 (8), 1163–74.

Ashburner, J., Friston, K. J., 2000. Voxel-based morphometry - the methods. Neuroimage 11, 805–21.

Bjuland, K. J., Løhaugen, G. C. C., Martinussen, M., Skranes, J., 2013. Cortical thickness and cognition in very-low-birth-weight late teenagers. Early Hum Dev 89 (6), 371–380.

Bland, J. M., Altman, D. G., 1986. Statistical methods for assessing agreement between two methods of clinical measurement. Lancet 327 (8476), 307–10.

Chen, C.-H., Gutierrez, E. D., Thompson, W., Panizzon, M. S., Jernigan, T. L., Eyler, L. T., Fennema-Notestine, C., Jak, A. J., Neale, M. C., Franz, C. E., Lyons, M. J., Grant, M. D., Fischl, B., Seidman, L. J., Tsuang, M. T., Kremen, W. S., Dale, A. M., 2012. Hierarchical genetic organization of human cortical surface area. Science 335 (6076), 1634–6.

Chen, C.-H., Panizzon, M. S., Eyler, L. T., Jernigan, T. L., Thompson, W., Fennema-Notestine, C., Jak, A. J., Neale, M. C., Franz, C. E., Hamza, S., Lyons, M. J., Grant, M. D., Fischl, B., Seidman, L. J., Tsuang, M. T., Kremen, W. S., Dale, A. M., 2011. Genetic influences on cortical regionalization in the human brain. Neuron 72 (4), 537–544.

Chen, C.-H., Peng, Q., Schork, A. J., Lo, M.-T., Fan, C.-C., Wang, Y., Desikan, R. S., Bettella, F., Hagler, D. J., Westlye, L. T., Kremen, W. S., Jernigan, T. L., Le Hellard, S., Steen, V. M., Espeseth, T., Huentelman, M., Håberg, A. K., Agartz, I., Djurovic, S., Andreassen, O. A., Schork, N., Dale, A. M., 2015. Large-scale genomics unveil polygenic architecture of human cortical surface area. Nature Communications 6 (May), 7549.

Dale, A. M., Fischl, B., Sereno, M. I., 1999. Cortical surface-based analysis I: Segmentation and surface reconstruction. Neuroimage 9 (2), 179–94.

Dale, A. M., Sereno, M. I., 1993. Improved localization of cortical activity by combining EEG and MEG with MRI cortical surface reconstruction. J Cogn Neurosci 5 (2), 162–176.

Davatzikos, C., 2004. Why voxel-based morphometric analysis should be used with great caution when characterizing group differences. NeuroImage 23 (1), 17–20.

Douaud, G., Smith, S., Jenkinson, M., Behrens, T., Johansen-Berg, H., Vickers, J., James, S., Voets, N., Watkins, K., Matthews, P. M., James, A., 2007. Anatomically related grey and white matter abnormalities in adolescent-onset schizophrenia. Brain 130 (9), 2375–2386.

Eikenes, L., Løhaugen, G. C., Brubakk, A. M., Skranes, J., Håberg, A. K., 2011. Young adults born preterm with very low birth weight demonstrate widespread white matter alterations on brain DTI. Neuroimage 54 (3), 1774–1785.

Fischl, B., Dale, A. M., 2000. Measuring the thickness of the human cerebral cortex from magnetic resonance images. Proc Natl Acad Sci USA 97 (20), 11050–5.

Fischl, B., Liu, A., Dale, A. M., 2001. Automated manifold surgery: constructing geometrically accurate and topologically correct models of the human cerebral cortex. IEEE Trans Med Imaging 20 (1), 70–80.

Fischl, B., Sereno, M. I., Dale, A. M., 1999a. Cortical surface-based analysis II: Inflation, flattening, and a surface-based coordinate system. Neuroimage 9 (2), 195–207.

Fischl, B., Sereno, M. I., Tootell, R. B., Dale, A. M., 1999b. High-resolution intersubject averaging and a coordinate system for the cortical surface. Hum Brain Mapp 8 (4), 272–84.

Fisher, R. A., 1932. Statistical Methods for Research Workers. Oliver and Boyd, Edinburgh.

Fjell, A. M., Grydeland, H., Krogsrud, S. K., Amlien, I., Rohani, D. A., Ferschmann, L., Storsve, A. B., Tamnes, C. K., Sala-Llonch, R., Due-Tønnessen, P., Bjørnerud, A., Sølsnes, A. E., Håberg, A. K., Skranes, J., Bartsch, H., Chen, C.-H., Thompson, W. K., Panizzon, M. S., Kremen, W. S., Dale, A. M., Walhovd, K. B., dec 2015. Development and aging of cortical thickness correspond to genetic organization patterns. Proc Natl Acad Sci USA 112 (50), 15462–15467.

Geschwind, D. H., Rakic, P., 2013. Cortical evolution: judge the brain by its cover. Neuron 80 (3), 633–47.

Glasser, M. F., Coalson, T. S., Robinson, E. C., Hacker, C. D., Harwell, J., Yacoub, E., Ugurbil, K., Andersson, J., Beckmann, C. F., Jenkinson, M., Smith, S. M., Van Essen, D. C., 2016. A multi-modal parcellation of human cerebral cortex. Nature 536 (7615), 171–8.

Glasser, M. F., Van Essen, D. C., 2011. Mapping human cortical areas in vivo based on myelin content as revealed by T1- and T2-weighted MRI. J Neurosci 31 (32), 11597–616.

Good, C. D., Johnsrude, I. S., Ashburner, J., Henson, R. N., Friston, K. J., Frackowiak, R. S., 2001. A voxel-based morphometric study of ageing in 465 normal adult human brains. Neuroimage 14 (1 Pt 1), 21–36.

Grunewaldt, K. H., Fjørtoft, T., Bjuland, K. J., Brubakk, A.-M., Eikenes, L., Håberg, A. K., Løhaugen, G. C. C., Skranes, J., 2014. Follow-up at age 10 years in ELBW children - functional outcome, brain morphology and results from motor assessments in infancy. Early Hum Dev 90 (10), 571–8.

Hagberg, H., Mallard, C., Ferriero, D. M., Vannucci, S. J., Levison, S. W., Vexler, Z. S., Gressens, P., 2015. The role of inflammation in perinatal brain injury. Nat Rev Neurol 11 (4), 192–208.

Harrison, N. A., Cooper, E., Dowell, N. G., Keramida, G., Voon, V., Critchley, H. D., Cercignani, M., 2015. Quantitative magnetization transfer imaging as a biomarker for effects of systemic inflammation on the brain. Biol Psychiatry 78 (1), 49–57.

Hill, J., Inder, T., Neil, J., Dierker, D., Harwell, J., van Essen, D., 2010. Similar patterns of cortical expansion during human development and evolution. Proc Natl Acad Sci

USA 107 (29), 13135–40.

Hogstrom, L. J., Westlye, L. T., Walhovd, K. B., Fjell, A. M., 2013. The structure of the cerebral cortex across adult life: age-related patterns of surface area, thickness, and gyrification. Cereb Cortex 23 (11), 2521–30.

Joyner, A. H., Roddey, J. C., Bloss, C. S., Bakken, T. E., Rimol, L. M., Melle, I., Agartz, I., Djurovic, S., Topol, E. J., Schork, N. J., Andreassen, O. A., Dale, A. M., 2009. A common MECP2 haplotype associates with reduced cortical surface area in humans in two independent populations. Proc Natl Acad Sci USA 106 (36), 15483–8.

Kenner, H., 1976. Geodesic math and how to use it. University of California Press, Los Angeles, CA, USA.

Kim, J. S., Singh, V., Lee, J. K., Lerch, J., Ad-Dab'bagh, Y., MacDonald, D., Lee, J. M., Kim, S. I., Evans, A. C., 2005. Automated 3-D extraction and evaluation of the inner and outer cortical surfaces using a Laplacian map and partial volume effect classification. Neuroimage 27 (1), 210–21.

Leahy, R. M., Qi, J., 2000. Statistical approaches in quantitative positron emission tomography. Stat Comput 10 (2), 147–165.

Lee, N. R., Adeyemi, E. I., Lin, A., Clasen, L. S., Lalonde, F. M., Condon, E., Driver, D. I., Shaw, P., Gogtay, N., Raznahan, A., Giedd, J. N., 2016. Dissociations in cortical morphometry in youth with down syndrome: Evidence for reduced surface area but increased thickness. Cerebral Cortex 26 (7), 2982–2990.

Lenroot, R. K., Schmitt, J. E., Ordaz, S. J., Wallace, G. L., Neale, M. C., Lerch, J. P., Kendler, K. S., Evans, A. C., Giedd, J. N., 2009. Differences in genetic and environmental influences on the human cerebral cortex associated with development during childhood and adolescence. Hum Brain Mapp 30 (1), 163–74.

Levesque, I. R., Giacomini, P. S., Narayanan, S., Ribeiro, L. T., Sled, J. G., Arnold, D. L., Pike, G. B., 2010. Quantitative magnetization transfer and myelin water imaging of the evolution of acute multiple sclerosis lesions. Magn Reson Med 63 (3), 633–640.

Lyttelton, O. C., Karama, S., Ad-Dab'bagh, Y., Zatorre, R. J., Carbonell, F., Worsley, K., Evans, A. C., 2009. Positional and surface area asymmetry of the human cerebral cortex. Neuroimage 46 (4), 895–903.

Mangin, J.-F., Frouin, V., Bloch, I., Regis, J., Lopes-Krabe, J., 1995. From 3D MR images to structural representations of the cortex topography using topology preserving deformations. Journal of Mathematical Imaging and Vision 5, 297–318.

Mangin, J.-F., Rivière, D., Cachia, A., Duchesnay, E., Cointepas, Y., Papadopoulos-Orfanos, D., Scifo, P., Ochiai, T., Brunelle, F., Régis, J., 2004. A framework to study the cortical folding patterns. NeuroImage 23 Suppl 1, S129–38.

Marín-Padilla, M., 1997. Developmental neuropathology and impact of perinatal brain damage. II: white matter lesions of the neocortex. J Neuropathol Exp Neurol 56 (3), 219–35.

Markoff, J., Shapiro, G., 1973. The linkage of data describing overlapping geographical units. Hist Methods Newsl 7 (1), 34–46.

Martinussen, M., Fischl, B., Larsson, H. B., Skranes, J., Kulseng, S., Vangberg, T. R., Vik, T., Brubakk, A. M., Haraldseth, O., Dale, A. M., 2005. Cerebral cortex thickness in 15-year-old adolescents with low birth weight measured by an automated MRI-based method. Brain 128 (11), 2588–2596.

Nichols, T., Brett, M., Andersson, J., Wager, T., Poline, J.-B., 2005. Valid conjunction inference with the minimum statistic. NeuroImage 25 (3), 653–60.

Noble, K. G., Houston, S. M., Brito, N. H., Bartsch, H., Kan, E., Kuperman, J. M., Akshoomoff, N., Amaral, D. G., Bloss, C. S., Libiger, O., Schork, N. J., Murray, S. S., Casey, B. J., Chang, L., Ernst, T. M., Frazier, J. A., Gruen, J. R., Kennedy, D. N., Van Zijl, P., Mostofsky, S., Kaufmann, W. E., Kenet, T., Dale, A. M., Jernigan, T. L., Sowell, E. R., 2015. Family income, parental education and brain structure in children and adolescents. Nat Neurosci 18 (5), 773–778.

O'Leary, D. D. M., Chou, S.-J., Sahara, S., 2007. Area patterning of the mammalian cortex. Neuron 56 (2), 252–69.

Palaniyappan, L., Mallikarjun, P., Joseph, V., White, T. P., Liddle, P. F., 2011. Regional contraction of brain surface area involves three large-scale networks in schizophrenia. Schizophr Res 129 (2-3), 163–8.

Panizzon, M. S., Fennema-Notestine, C., Eyler, L. T., Jernigan, T. L., Prom-Wormley, E., Neale, M., Jacobson, K., Lyons, M. J., Grant, M. D., Franz, C. E., Xian, H., Tsuang,

M., Fischl, B., Seidman, L., Dale, A., Kremen, W. S., 2009. Distinct genetic influences on cortical surface area and cortical thickness. Cereb Cortex 19 (11), 2728–35.

Pantazis, D., Nichols, T. E., Baillet, S., Leahy, R. M., 2005. A comparison of random field theory and permutation methods for the statistical analysis of MEG data. Neuroimage 25 (2), 383–94.

Parker, G. J. M., Padhani, A. R., 2003. T_1-w DCE-MRI: T_1-weighted Dynamic Contrast-Enhanced MRI. In: Tofts, P. (Ed.), Quantitative MRI of the Brain: Measuring Changes Caused by Disease. John Wiley & Sons, pp. 341–364.

Pesarin, F., Salmaso, L., 2010. Permutation Tests for Complex Data: Theory, Applications and Software. John Wiley and Sons, West Sussex, England, UK.

Rakic, P., 1988. Specification of cerebral cortical areas. Science 241 (4862), 170–6.

Rakic, P., sep 1995. A small step for the cell, a giant leap for mankind: a hypothesis of neocortical expansion during evolution. Trends Neurosci 18 (9), 383–8.

Raznahan, A., Shaw, P., Lalonde, F., Stockman, M., Wallace, G. L., Greenstein, D., Clasen, L., Gogtay, N., Giedd, J. N., 2011. How does your cortex grow? J Neurosci 31 (19), 7174–7.

Rimol, L. M., Agartz, I., Djurovic, S., Brown, A. A., Roddey, J. C., Kähler, A. K., Mattingsdal, M., Athanasiu, L., Joyner, A. H., Schork, N. J., Halgren, E., Sundet, K., Melle, I., Dale, A. M., Andreassen, O. A., Alzheimer's Disease Neuroimaging Initiative, 2010a. Sex-dependent association of common variants of microcephaly genes with brain structure. Proc Natl Acad Sci USA 107 (1), 384–8.

Rimol, L. M., Bjuland, K. J., Løhaugen, G. C. C., Martinussen, M., Evensen, K. A. I., Indredavik, M. S., Brubakk, A.-M., Eikenes, L., Håberg, A. K., Skranes, J., 2016. Cortical trajectories during adolescence in preterm born teenagers with very low birthweight. Cortex 75, 120–31.

Rimol, L. M., Nesvå g, R., Hagler, D. J., Bergmann, O., Fennema-Notestine, C., Hartberg, C. B., Haukvik, U. K., Lange, E., Pung, C. J., Server, A., Melle, I., Andreassen, O. A., Agartz, I., Dale, A. M., 2012. Cortical volume, surface area, and thickness in schizophrenia and bipolar disorder. Biol Psychiatry 71 (6), 552–60.

Rimol, L. M., Panizzon, M. S., Fennema-Notestine, C., Eyler, L. T., Fischl, B., Franz, C. E., Hagler, D. J., Lyons, M. J., Neale, M. C., Pacheco, J., Perry, M. E., Schmitt, J. E., Grant, M. D., Seidman, L. J., Thermenos, H. W., Tsuang, M. T., Eisen, S. A., Kremen, W. S., Dale, A. M., 2010b. Cortical thickness is influenced by regionally specific genetic factors. Biol Psychiatry 67 (5), 493–9.

Robinson, E. C., Jbabdi, S., Glasser, M. F., Andersson, J., Burgess, G. C., Harms, M. P., Smith, S. M., Van Essen, D. C., Jenkinson, M., 2014. MSM: A new flexible framework for multimodal surface matching. Neuroimage 100, 414–26.

Roy, S. N., Jun. 1953. On a heuristic method of test construction and its use in multivariate analysis. Ann Math Stat 24 (2), 220–238.

Saad, Z. S., Reynolds, R. C., Argall, B., Japee, S., Cox, R. W., 2004. SUMA: An interface for surface-based intra- and inter-subject analysis with AFNI. IEEE International Symposium on Biomedical Imaging, 1510–1513.

Schaer, M., Cuadra, M. B., Tamarit, L., Lazeyras, F., Eliez, S., Thiran, J.-P., 2008. A surface-based approach to quantify local cortical gyrification. IEEE Trans Med Imaging 27 (2), 161–70.

Schmitt, J. E., Lenroot, R. K., Wallace, G. L., Ordaz, S., Taylor, K. N., Kabani, N. J., Greenstein, D., Lerch, J. P., Kendler, K. S., Neale, M. C., Giedd, J. N., 2008. Identification of genetically mediated cortical networks: a multivariate study of pediatric twins and siblings. Cereb Cortex 18 (8), 1737–47.

Schnack, H. G., Van Haren, N. E. M., Brouwer, R. M., Evans, A., Durston, S., Boomsma, D. I., Kahn, R. S., Hulshoff Pol, H. E., 2015. Changes in thickness and surface area of the human cortex and their relationship with intelligence. Cereb Cortex 25 (6), 1608–1617.

Ségonne, F., Dale, A. M., Busa, E., Glessner, M., Salat, D., Hahn, H. K., Fischl, B., 2004. A hybrid approach to the skull stripping problem in MRI. Neuroimage 22 (3), 1060–75.

Ségonne, F., Pacheco, J., Fischl, B., 2007. Geometrically accurate topology-correction of cortical surfaces using nonseparating loops. IEEE Trans Med Imaging 26 (4), 518–29.

Sereno, M. I., Lutti, A., Weiskopf, N., Dick, F., 2013. Mapping the human cortical surface by combining quantitative T1 with retinotopy. Cereb Cortex 23 (9), 2261–8.

Skranes, J., Løhaugen, G. C. C., Martinussen, M., Håberg, A., Brubakk, A. M., Dale,

A. M., 2013. Cortical surface area and IQ in very-low-birth-weight (VLBW) young adults. Cortex 49 (8), 2264–2271.

Skranes, J., Vangberg, T. R., Kulseng, S., Indredavik, M. S., Evensen, K. A. I., Martinussen, M., Dale, A. M., Haraldseth, O., Brubakk, A. M., 2007. Clinical findings and white matter abnormalities seen on diffusion tensor imaging in adolescents with very low birth weight. Brain 130 (3), 654–666.

Sølsnes, A. E., Grunewaldt, K. H., Bjuland, K. J., Stavnes, E. M., Bastholm, I. a., Aanes, S., Østgård, H. F., Håberg, A., Løhaugen, G. C. C., Skranes, J., Rimol, L. M., 2015. Cortical morphometry and IQ in VLBW children without cerebral palsy born in 2003-2007. Neuroimage. Clinical 8, 193–201.

Storsve, A. B., Fjell, A. M., Tamnes, C. K., Westlye, L. T., Overbye, K., Aasland, H. W., Walhovd, K. B., 2014. Differential longitudinal changes in cortical thickness, surface area and volume across the adult life span: regions of accelerating and decelerating change. The Journal of Neuroscience 34 (25), 8488–98.

Stouffer, S. A., Suchman, E. A., DeVinney, L. C., Star, S. A., Jr., R. M. W., 1949. The American Soldier: Adjustment During Army Life (Volume 1). Princeton University Press, Princeton, New Jersey, USA.

Sun, D., Phillips, L., Velakoulis, D., Yung, A., McGorry, P. D., Wood, S. J., van Erp, T. G. M., Thompson, P. M., Toga, A. W., Cannon, T. D., Pantelis, C., 2009a. Progressive brain structural changes mapped as psychosis develops in 'at risk' individuals. Schizophr Res 108 (1-3), 85–92.

Sun, D., Stuart, G. W., Jenkinson, M., Wood, S. J., McGorry, P. D., Velakoulis, D., van Erp, T. G. M., Thompson, P. M., Toga, a. W., Smith, D. J., Cannon, T. D., Pantelis, C., 2009b. Brain surface contraction mapped in first-episode schizophrenia: a longitudinal magnetic resonance imaging study. Mol Psychiatry 14 (10), 976–86.

Tallinen, T., Chung, J. Y., Biggins, J. S., Mahadevan, L., 2014. Gyrification from constrained cortical expansion. Proc Natl Acad Sci USA 111 (35), 12667–72.

Tallinen, T., Chung, J. Y., Rousseau, F., Girard, N., Lefèvre, J., Mahadevan, L., 2016. On the growth and form of cortical convolutions. Nature Phys 12 (6), 588–593.

Toro, R., Perron, M., Pike, B., Richer, L., Veillette, S., Pausova, Z., Paus, T., 2008. Brain size and folding of the human cerebral cortex. Cereb Cortex 18 (10), 2352–7.

van den Hoff, J., 2005. Principles of quantitative positron emission tomography. Amino Acids 29 (4), 341–53.

van Essen, D. C., 2005. A Population-Average, Landmark- and Surface-based (PALS) atlas of human cerebral cortex. Neuroimage 28 (3), 635–62.

van Essen, D. C., Drury, H. A., Dickson, J., Harwell, J., Hanlon, D., Anderson, C. H., 2001. An integrated software suite for surface-based analyses of cerebral cortex. Journal of American Medical Informatics Association 8 (5), 443–59.

Voets, N. L., Hough, M. G., Douaud, G., Matthews, P. M., James, A., Winmill, L., Webster, P., Smith, S., 2008. Evidence for abnormalities of cortical development in adolescent-onset schizophrenia. Neuroimage 43 (4), 665–75.

Volpe, J. J., 2009. Brain injury in premature infants: a complex amalgam of destructive and developmental disturbances. Lancet Neurol 8 (1), 110–124.

Volpe, J. J., 2011. Systemic inflammation, oligodendroglial maturation, and the encephalopathy of prematurity. Ann Neurol 70 (4), 525–529.

Vuoksimaa, E., Panizzon, M. S., Chen, C.-H., Fiecas, M., Eyler, L. T., Fennema-Notestine, C., Hagler, D. J., Franz, C. E., Jak, A. J., Lyons, M. J., Neale, M. C., Rinker, D. A., Thompson, W. K., Tsuang, M. T., Dale, A. M., Kremen, W. S., 2016. Is bigger always better? the importance of cortical configuration with respect to cognitive ability. Neuroimage 129, 356–366.

Westfall, P. H., Young, S. S., 1993. Resampling-Based Multiple Testing: Examples And Methods for p-Value Adjustment. John Wiley and Sons, New York.

Winkler, A. M., Kochunov, P., Blangero, J., Almasy, L., Zilles, K., Fox, P. T., Duggirala, R., Glahn, D. C., 2010. Cortical thickness or grey matter volume? The importance of selecting the phenotype for imaging genetics studies. Neuroimage 15 (3), 1135–46.

Winkler, A. M., Ridgway, G. R., Douaud, G., Nichols, T. E., Smith, S. M., 2016a. Faster permutation inference in brain imaging. NeuroImage 141, 502–516.

Winkler, A. M., Ridgway, G. R., Webster, M. A., Smith, S. M., Nichols, T. E., 2014. Permutation inference for the general linear model. Neuroimage 92, 381–97.

Winkler, A. M., Sabuncu, M. R., Yeo, B. T. T., Fischl, B., Greve, D. N., Kochunov,

P., Nichols, T. E., Blangero, J., Glahn, D. C., 2012. Measuring and comparing brain cortical surface area and other areal quantities. Neuroimage 61 (4), 1428–43.

Winkler, A. M., Webster, M. A., Brooks, J. C., Tracey, I., Smith, S. M., Nichols, T. E., 2016b. Non-Parametric Combination and related permutation tests for neuroimaging. Hum Brain Mapp 37 (4), 1486–511.

Winkler, A. M., Webster, M. A., Vidaurre, D., Nichols, T. E., Smith, S. M., 2015. Multi-level block permutation. Neuroimage 123, 253–68.

Yeo, B. T., Sabuncu, M. R., Vercauteren, T., Ayache, N., Fischl, B., Golland, P., 2010. Spherical demons: fast diffeomorphic landmark-free surface registration. IEEE Trans Med Imaging 29 (3), 650–68.